

## Invited Review

# Mechanisms of GTP Hydrolysis and Conformational Transitions in the Dynamin Superfamily

Oliver Daumke,<sup>1,2</sup> Gerrit J. K. Praefcke<sup>3</sup>

<sup>1</sup> Kristallographie, Max-Delbrück Centrum Für Molekulare Medizin, Robert-Rössle-Straße 10, Berlin 13125, Germany

<sup>2</sup> Institut Für Chemie und Biochemie, Freie Universität Berlin, Takustraße 3, Berlin 14195, Germany

<sup>3</sup> Abteilung Hämatologie/Transfusionsmedizin, Paul-Ehrlich-Institut, Paul-Ehrlich-Straße 51-59, Langen 63225, Germany

Received 14 January 2016; revised 31 March 2016; accepted 1 April 2016

Published online 8 April 2016 in Wiley Online Library (wileyonlinelibrary.com). DOI 10.1002/bip.22855

### ABSTRACT:

Dynamin superfamily proteins are multidomain mechano-chemical GTPases which are implicated in nucleotide-dependent membrane remodeling events. A prominent feature of these proteins is their assembly-stimulated mechanism of GTP hydrolysis. The molecular basis for this reaction has been initially clarified for the dynamin-related guanylate binding protein 1 (GBP1) and involves the transient dimerization of the GTPase domains in a parallel head-to-head fashion. A catalytic arginine finger from the phosphate binding (P-) loop is repositioned toward the nucleotide of the same molecule to stabilize the transition state of GTP hydrolysis. Dynamin uses a related dimerization-dependent mechanism, but instead of the catalytic arginine, a monovalent cation is involved in catalysis. Still another variation of the GTP hydrolysis mechanism has been revealed for the dynamin-like Irga6 which bears a glycine at the corresponding position in the P-loop. Here, we highlight conserved and divergent features of GTP hydrolysis in dynamin superfamily proteins and show how nucleotide

binding and hydrolysis are converted into mechano-chemical movements. We also describe models how the energy of GTP hydrolysis can be harnessed for diverse membrane remodeling events, such as membrane fission or fusion. © 2016 The Authors. Biopolymers Published by Wiley Periodicals, Inc. *Biopolymers* 105: 580–593, 2016.  
**Keywords:** dynamin; GTPases; structural biology; catalytic mechanism; mechanochemical enzyme

This article was originally published online as an accepted preprint. The “Published Online” date corresponds to the preprint version. You can request a copy of any preprints from the past two calendar years by emailing the Biopolymers editorial office at [biopolymers@wiley.com](mailto:biopolymers@wiley.com).

### INTRODUCTION

Proteins of the dynamin superfamily utilize the energy of GTP hydrolysis to perform some type of mechanical work which is mostly exploited for the remodeling of cellular membranes.<sup>1,2</sup> Therefore, these proteins are considered as mechano-chemical enzymes. The first cloned dynamin superfamily gene was that of the interferon-inducible myxovirus resistance (Mx) gene.<sup>3</sup> Shortly after, a gene with related sequence, VPS1, was identified due to its role in vacuolar sorting in yeast.<sup>4</sup> In 1989, the protein dynamin was discovered as a microtubule-associated protein.<sup>5</sup> Subsequently, the dynamin gene was cloned from a rat brain cDNA library<sup>6</sup> and was shown to correspond to the *Drosophila shibire* locus.<sup>7,8</sup> Temperature-

This is an open access article under the terms of the Creative Commons Attribution-NonCommercial-NoDerivs License, which permits use and distribution in any medium, provided the original work is properly cited, the use is non-commercial and no modifications or adaptations are made.

Correspondence to: Oliver Daumke; e-mail: [oliver.daumke@mdc-berlin.de](mailto:oliver.daumke@mdc-berlin.de) or Gerrit J. K. Praefcke; e-mail: [gerrit.praefcke@pei.de](mailto:gerrit.praefcke@pei.de)

© 2016 The Authors. *Biopolymers* Published by Wiley Periodicals, Inc.

sensitive alleles of *shibire* were known to affect endocytosis at the fly synapse resulting in paralysis due to depletion of synaptic vesicles.<sup>9,10</sup> Today, dynamin is well-known for its function in catalyzing the scission of clathrin-coated vesicles from the plasma membrane (reviewed in Ref. 11).

Several additional members of the dynamin superfamily have been identified over the years: Dynamin-1-like protein (DNM1L) is implicated in the scission of mitochondria.<sup>12</sup> Optic atrophy type 1 (OPA1 or mitochondrial genome maintenance protein 1/Mgm1p in yeast) mediates the fusion of the inner mitochondrial membrane and is involved in cristae formation,<sup>13–16</sup> whereas mitofusins/fuzzy onions (Fzo1p) execute the fusion of the outer mitochondrial membrane.<sup>17,18</sup> Besides the Mx proteins, also the dynamin-related guanylate binding proteins (GBPs) and the 47 kD immunity-related GTPases (IRGs) are induced by interferons.<sup>19,20</sup> GBPs mediate immunity against several microbial and viral pathogens, but also regulate cell adhesion and migration,<sup>21</sup> whereas IRGs are best characterized in mice and were shown to convey the clearance of intracellular pathogens, such as *Toxoplasma gondii*.<sup>22</sup> Atlantins/Sey1p are phylogenetically most closely related to GBPs and catalyze the fusion of endoplasmic reticulum (ER) tubules in higher eukaryotes and yeast, respectively.<sup>23,24</sup> A family of dynamin-related ATPases, the Eps15-homology domain containing proteins (EHDs), are involved in various membrane trafficking pathways originating from the plasma membrane or from internal membrane systems.<sup>25</sup> Dynamin-related proteins were also identified in bacteria, where they are thought to mediate bacterial membrane remodeling events, for example, during cell or thylakoid division.<sup>26,27</sup> Furthermore, dynamin-like LeoA from a pathogenic *E. coli* strain has been assigned a role in the secretion of bacterial vesicles for enhancing the release of toxins.<sup>28</sup>

In this article, we introduce structural features of dynamin superfamily proteins and explain their various mechanisms of GTP hydrolysis, using GBP1, dynamin and Irga6 as examples. We show for selected members how GTP hydrolysis is converted into a large-scale conformational change of the adjacent helical bundle. Furthermore, we explain models how the energy of GTP hydrolysis is exploited for various membrane remodeling events.

## COMMON BIOCHEMICAL AND STRUCTURAL FEATURES OF DYNAMIN SUPERFAMILY PROTEINS

A unifying feature of dynamin superfamily protein is their ability to assemble into regular oligomers on appropriate templates. For example, dynamin can self-assemble around microtubules or the neck of clathrin-coated vesicles into regu-

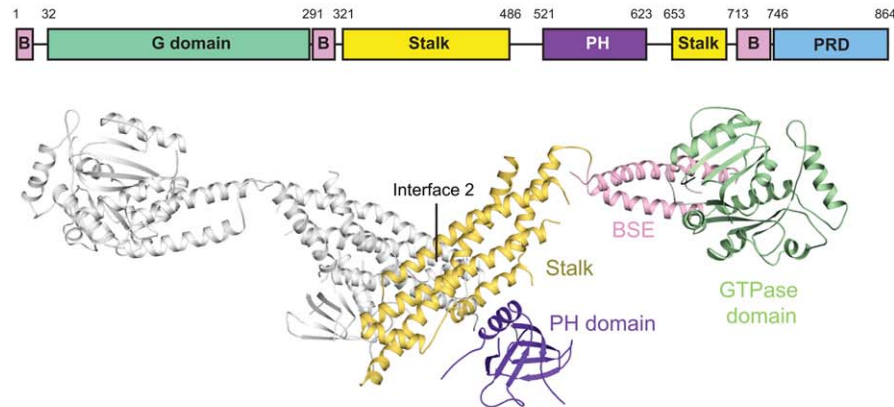
lar rings or helices.<sup>29</sup> Similar ring-like or helical structures can be reconstituted in vitro using artificial tubular membrane templates.<sup>30–32</sup> Also MxA,<sup>33,34</sup> DNM1L,<sup>35,36</sup> EHD2,<sup>37</sup> OPA1,<sup>38</sup> and BDLP<sup>39</sup> can form helical oligomers on the surface of membranes.

Due to their low nucleotide affinities, dynamin superfamily members do not require guanine nucleotide exchange factors for catalyzing nucleotide release. Furthermore, they display a relatively high basal rate of GTP hydrolysis. For example, dynamin, MxA and GBP1 have basal GTP hydrolysis rates of 1–5 min<sup>-1</sup> at 37°C.<sup>40–42</sup> These rates cooperatively increase with the protein concentration.<sup>41,43–45</sup> In the presence of appropriate templates, the GTPase activity can be further enhanced, for example, for dynamin, a >100-fold increase in GTPase rate was observed in the presence of tubular membrane templates.<sup>31,46</sup> Thus, GTPase activities of unassembled dynamin superfamily proteins are often inhibited in solution, and auto-inhibitory restraints are relieved when the proteins are recruited to their physiological site of action.

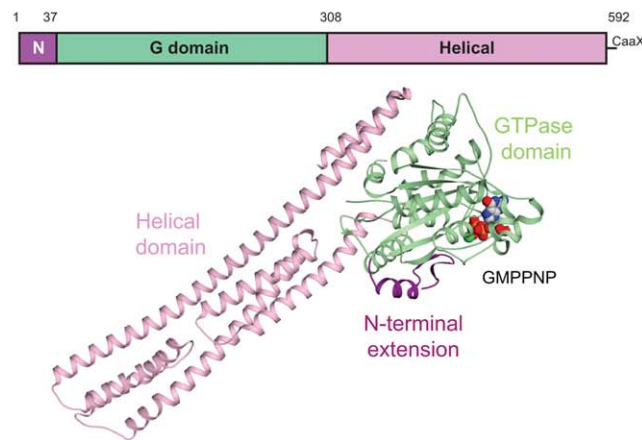
Recent full-length or almost full-length crystal structures of dynamin,<sup>47–49</sup> MxA,<sup>50</sup> MxB,<sup>51</sup> DNM1L,<sup>52</sup> GBP1,<sup>44,53</sup> atlantins,<sup>54–56</sup> Irga6,<sup>57,58</sup> Sey1p,<sup>59</sup> EHD2,<sup>37</sup> BDLP,<sup>26</sup> and LeoA<sup>28</sup> have revealed the architecture of dynamin superfamily proteins (Figure 1). The most highly conserved region in these proteins is their amino-terminal extended or large GTPase domain. Thus, dynamin's GTPase domain has various insertions compared to the Ras-like minimal GTPase domains,<sup>61</sup> which are also found in the closely related MxA and DNM1L. In the more distantly related GBP1, atlantins, EHD2 and BDLP, these extensions differ in length and position. Consequently, the typical size of a GTPase domain in dynamin superfamily proteins comprises about 300 residues, compared to 170 residues in Ras-like GTP-binding proteins.

As in many regulatory GTP-binding proteins, five motifs in the GTPase domain (G1–G5) are involved in nucleotide-binding (Figure 2A).<sup>63</sup> The G1 motif forms the P-loop with the consensus GxxxxGKS/T. It tightly wraps around the  $\beta$ -phosphate and contributes with the terminal serine/threonine to the binding of a Mg<sup>2+</sup> ion which is crucial for GTP hydrolysis in many ATPases and GTPases. Also a direct contact of the conserved Thr of the G2 motif and a direct or water-mediated contact by the conserved Asp in the G3 motif participate in Mg<sup>2+</sup>-binding. In addition, residues in these motifs directly contact the  $\gamma$ -phosphate. Accordingly, the two regions encompassing these motifs undergo  $\gamma$ -phosphate-dependent conformational changes and have therefore been termed the switch regions. Compared to Ras-like GTPases, dynamin superfamily proteins do not possess a catalytic glutamine following the G3 motif, but instead a hydrophobic residue. In GBP1, this Leu101 points away from the

### A Dynamin



### B GBP1



### C EHD2

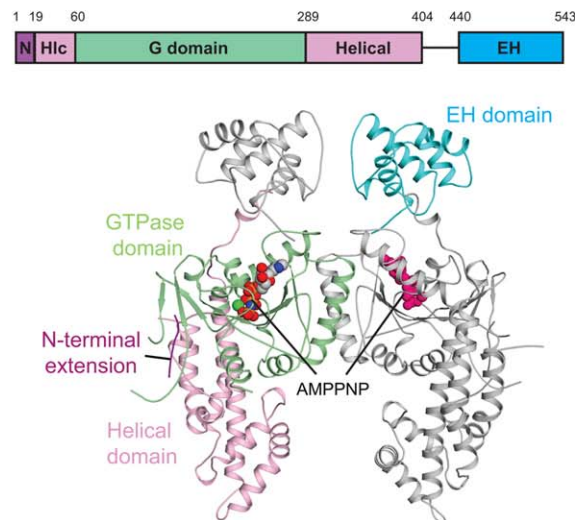


**FIGURE 1** Domain architecture of selected dynamin superfamily proteins. (A) In the schematic domain architecture, numbers refer to the amino acid sequence of human dynamin 1. The crystal structure of the nucleotide-free dynamin 1 dimer (pdb 3SNH)<sup>47</sup> shows a four domain architecture. Stable dimerization is mediated via the highly conserved stalk interface-2. The PRD was not present in the crystallized construct. MxA<sup>50</sup> and DNML1<sup>52</sup> show a highly related structure and assembly mode. (B) Domain architecture of human GBP1 and crystal structure of the GMPPNP-loaded monomer (pdb 1F5N).<sup>53</sup> The flexible C-terminus carrying the farnesylation site (CaaX) was not resolved in the structure. (C) Domain architecture of murine EHD2 and structure of the AMPPNP-bound EHD2 dimer (pdb 4CID).<sup>60</sup>

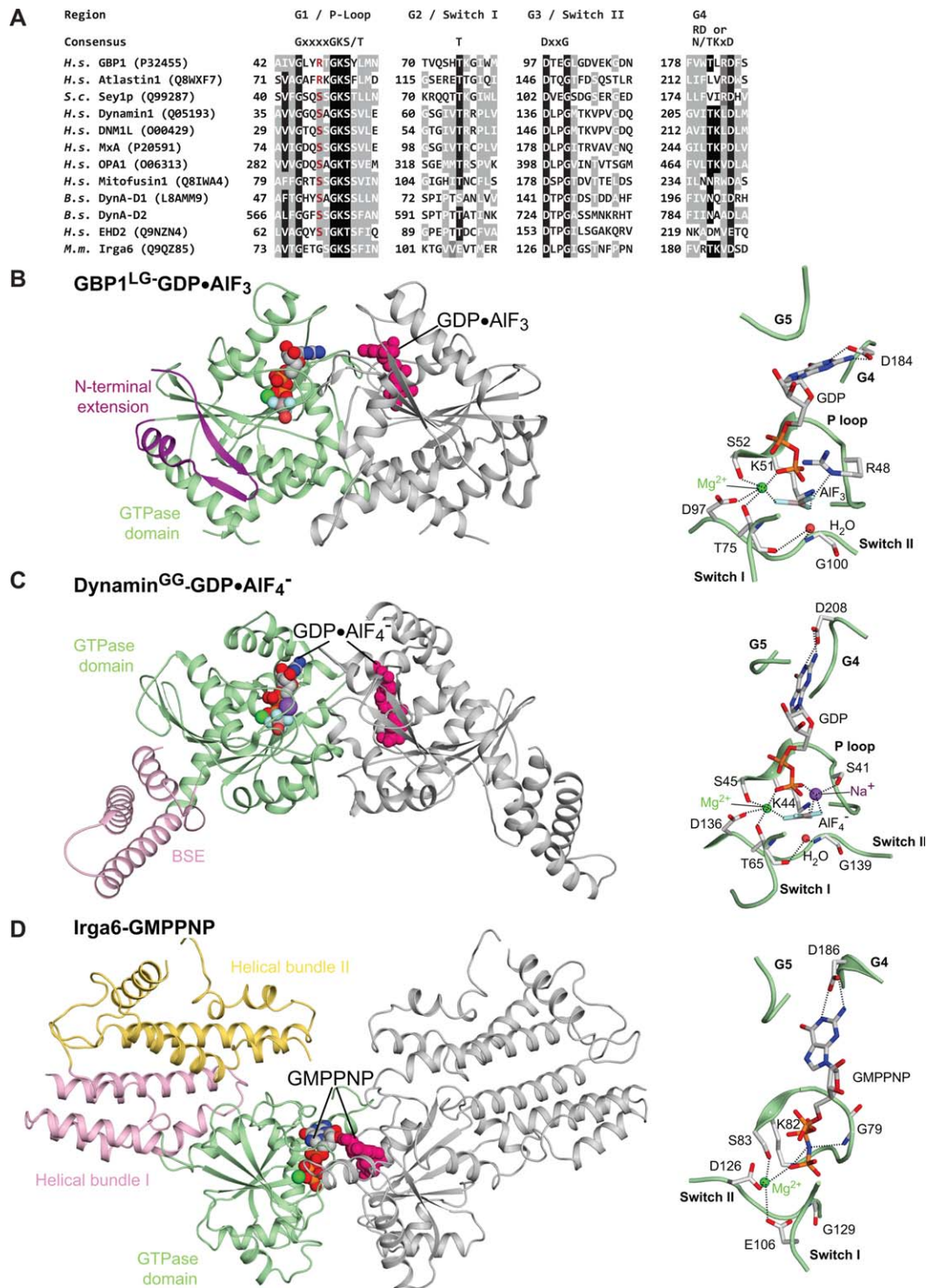


**FIGURE 2** Catalytic mechanism of dynamin superfamily proteins. (A) Sequence alignment of dynamin superfamily proteins in the G1–G4 motifs. Conserved canonical residues are highlighted in black or dark gray, other conserved residues in light grey. The catalytic arginine and serines in the P-loop are shown in red. For DynA from *B. subtilis*, the sequence of both GTPase domains is shown. (B–D) Dynamin superfamily proteins activate their GTPase by dimerizing in a parallel, head-to-head fashion. This leads to rearrangement of catalytic residues *in cis*. Mg<sup>2+</sup>-ions are shown as green and Na<sup>+</sup>-ions as purple spheres. (B) The GDP-AlF<sub>3</sub> bound LG-domain dimer of hGBP1 (pdb 2B92).<sup>42</sup> (C) The GDP-AlF<sub>4</sub><sup>-</sup>-bound GG construct of dynamin (pdb 2X2E).<sup>62</sup> (D) GMPPNP-bound Irga6 (pdb 5FPH). Due to expression in *E. coli*, the protein lacks the N-terminal myristoylation. At the right, details of the interactions of the G1–G5 motifs in the catalytic site are shown, with hydrogen bonds indicated by dashed lines. The Na<sup>+</sup>-ion in dynamin is additionally contacted by main chain contacts from Gly60 and Gly62 from switch I (not shown here).

nucleotide toward the hydrophobic core of the protein and may stabilize the conformation of switch II. Similar conformations were later shown for other dynamin proteins. An aspartate in the G4 motif mediates specific binding to the guanine base. The consensus N/TKxD is differently conserved as RD in GBPs and atlastins.<sup>54,55,64</sup> In EHD proteins, the conserved aspartate in G4 is engaged in auto-inhibitory interactions with the tail of the carboxy-(C-)terminal Eps15 homology domain (EH domain), and a methionine directly following the G4 motif sterically restricts binding of the amino group of the guanine base.<sup>37</sup> Consequently, EHDs use ATP instead of GTP as a substrate. Residues in the G5 motif are not well conserved between different dynamin families and interact in various ways with the guanine base and/or ribose.

The LG-domain is often followed by one or several helical bundles. Sometimes, these helical bundles include elements from the N-terminal region of the GTPase domain. For example, in the bundle signaling element (BSE) of dynamin and in the helical bundle of EHD2, one or two helices are derived from the N-terminal region, respectively (Figures 1A and 2C). The second helical element in dynamin is called the stalk. It was shown to mediate the assembly of dynamin, MxA and DNMI1 into a helical filament by providing three distinct assembly interfaces<sup>41,49,52</sup> (reviewed in ref. 2). The stalk provides additional regulatory interaction sites for the BSE (as shown for MxA and dynamin) and for the PH domain (as shown for dynamin).<sup>47,50</sup> Furthermore, based on crystal packing and mutagenesis, another conserved interface of the stalk has been suggested to mediate higher order assembly of DNMI1.<sup>52</sup> Interestingly, the position of this stalk interface corresponds to that of the PH domain binding site in dynamin (see also below), so alternative functions of this interaction site may be envisaged for the different members. In many cases, the C-terminal helix of the helical bundles folds back to the GTPase domain, allowing a tight coupling of nucleotide binding/hydrolysis and oligomerization.

In many dynamin superfamily members, the membrane binding site is located at the tip of the helical domain. For example, in dynamin, a specialized pleckstrin homology (PH) domain mediates the binding to phosphatidylinositol phosphates containing membranes, whereas Mx and DNMI1 have large, membrane-binding loop regions at this position<sup>34,36,52,65</sup> and EHD2 a polybasic helix.<sup>37</sup> Atlastin, mitofusin, and bacterial dynamin-like protein (BDLP) contain transmembrane sequences at the tip of their helical domains. One OPA1/Mgm1p isoform bears an N-terminal transmembrane sequence, which is, however, not required for efficient liposome binding and tubulation *in vitro*.<sup>66</sup> Instead, OPA1/Mgm1p may also contain a membrane-binding domain at the

tip of the stalk.<sup>67</sup> GBPs and IRGs have N- and C-terminal lipid attachment motifs, respectively.

Some dynamin superfamily members possess additional interaction domains or motifs. For example, a proline-/arginine-rich domain (PRD) at the C-terminus of dynamin mediates its recruitment to clathrin-coated pits by binding to Src-homology 3 (SH3) domain containing BAR (Bin-Amphiphysin-Rvs) domain proteins,<sup>68</sup> whereas an EH domain in EHDs is thought to regulate assembly and/or membrane recruitment by binding to linear Asn-Pro-Phe (NPF) motifs of target proteins (Figure 1).<sup>37</sup>

### GBP1 AND ATLASTIN1 EMPLOY AN INTERNAL ARGININE FINGER FOR GTP HYDROLYSIS

The mechanism of the stimulated GTPase reaction was first revealed for GBP1 using a combination of structural and biochemical studies with a truncated LG-domain construct.<sup>42</sup> This construct retains the basic properties of nucleotide-binding and cooperative GTP hydrolysis and dimerizes in the presence of GTP and GDP-AlF<sub>4</sub><sup>-</sup> and GMP-AlF<sub>4</sub><sup>-</sup>, but not in the absence of nucleotide or the presence of GMP. As a unique property, GBP1 can hydrolyze GTP in two consecutive cleavage reactions to GMP and the LG-domain dimerizes also in the presence of GMP-AlF<sub>4</sub><sup>-</sup>.<sup>42,69,70</sup>

X-ray structures of the truncated LG-domain construct were determined in the presence of a nonhydrolysable GTP analogue 5'-guanylyl imidodiphosphate (GMPPNP), the transition state analogues GDP-AlF<sub>4</sub><sup>-</sup>, GMP-AlF<sub>4</sub><sup>-</sup>, and GMP.<sup>42</sup> With the exception of the GMP-bound structure, all of the truncated LG-domain structures showed parallel head-to-head GTPase domain dimers (Figure 2B). The highly conserved dimerization surface, the G-interface, is formed across the nucleotide-binding site. This interface involves the P-loop, the two switch regions which are stabilized in the dimer, and several additional loop regions, including a loop following the G4 motif that directly contacts the guanine base of the opposing molecule. The switch I region interacts with another large loop, the guanine cap, which then binds *in trans* to the opposing monomer.<sup>71</sup> The ordering of the switch regions in the transition state structures leads to the repositioning of Thr75 from switch I which, via a main chain interaction and together with the adjacent Ser73, positions a catalytic water molecule (Figure 2B).<sup>42</sup>

A surprising involvement of the third residue in the P-loop, Arg48, was identified.<sup>42,45</sup> During dimerization, the side-chain of Arg48 rearranges toward the transition state mimic AlF<sub>4</sub><sup>-</sup> within the same molecule. It appears to stabilize the negative charge during the transition state of GTP hydrolysis and thus

acts as an internal catalytic arginine finger. Mutation of Arg48 did not abolish dimerization, but completely interfered with GTP hydrolysis while the S73A mutant displayed a strongly reduced and non-cooperative GTP hydrolysis. Interestingly, the complete catalytic machinery retained its positions in the GMP- $\text{AlF}_4^-$  bound structure, but the  $\alpha$ -phosphate of the GMP was shifted toward the position of the  $\beta$ -phosphate in the GDP- $\text{AlF}_4^-$  bound structure. This plasticity of nucleotide binding within the catalytic site appears to be a unique feature of GBP1 within the dynamain superfamily allowing it to employ the same set of catalytic residues for GTP and GDP hydrolysis.

A similar dimerization-dependent mechanism of GTP hydrolysis was found for the close relative of GBP1, atlastin. An atlastin1 construct encompassing the GTPase domain and three helices of the adjacent helical bundle was crystallized in two GDP-bound states,<sup>54,55</sup> and later, in the presence of GMPPNP and GDP- $\text{AlF}_4^-$ .<sup>56</sup> In all of these structures, atlastin dimerized via the G-interface, although only GMPPNP and GDP- $\text{AlF}_4^-$  led to stable dimerization in solution.<sup>54,55</sup> Also in this construct, the corresponding arginine from the P-loop stabilized the transition state of GTP hydrolysis. However, the arginine in atlastin may have a dual role since in the GDP-bound structures, it participates in the G-interface. Consequently, the R77E mutation impaired binding of GTP analogues and prevented GTP hydrolysis as well as dimerization,<sup>54,55</sup> whereas the R77A mutation interfered only with GTP hydrolysis.<sup>56</sup>

### DYNAMAIN EMPLOYS A CATALYTIC CATION FOR GTP HYDROLYSIS

The crystal structure of a dynamain GTPase domain construct including a truncated version of the adjacent BSE (the so-called GTPase-GED (GG) fusion protein) revealed the catalytic mechanism of GTP hydrolysis (Figure 2C).<sup>62</sup> In solution, GDP- $\text{AlF}_4^-$ , but no other nucleotide, promoted stable dimerization. Accordingly, the GDP- $\text{AlF}_4^-$ -bound GG-construct was found to dimerize in the crystals via the G-interface in a parallel head-to-head fashion. Similar to GBP1, both switch regions, the *trans* stabilizing loop and the dynamain-specific loop participate in the assembly. Furthermore, Asp211 from the G4-loop contacts the guanine base of the opposing molecule *in trans*. A catalytic water molecule is stabilized by a main chain interaction of Thr65 in switch I; Thr65 had previously been shown by mutational studies to be crucial for catalysis, but its mutation to alanine did not grossly affect nucleotide binding.<sup>72</sup> Importantly, a conserved serine (Ser41) from the third position in the P-loop corresponding to Arg48 in GBP1 and two glycines from switch I were demonstrated to interact with a monovalent catalytic cation (sodium or potassium) which directly contacts the  $\text{AlF}_4^-$  anion.<sup>62</sup> This cation was proposed to stabilize the transition

state of GTP hydrolysis in a similar manner as the equivalent arginine in GBP1. Sequence comparisons indicate that the serine is conserved in many dynamain superfamily proteins, such as DNM1L, Vps1p, MxA, mitochondrial OPA1 and mitofusin proteins, EHDs, and several bacterial dynamains (Figure 2A). Fzo1p from yeast and a few other dynamain family members display an Asn at the corresponding position which is reminiscent of the potassium-specific P-loop of MnME, a GTPase involved in tRNA modification.<sup>73</sup> This suggests that cation-dependent GTP hydrolysis may be a general feature of dynamain superfamily members, unless they carry an Arg in the P-loop, as seen in GBPs and atlastins.<sup>74</sup> However, the classification in cation- and Arg-dependent dynamain GTPases does not strictly follow evolutionary or functional conservation. Sey1p from yeast and RHD3 from *Arabidopsis thaliana* have a serine at the third position of the P-loop although sequence comparisons identify them as GBP/atlastin-related proteins.<sup>24,59</sup> Furthermore, some GBPs as well as the close atlastin-homologue neurotactin that has only recently been described as a dynamain homologue<sup>75</sup> have a histidine at the respective position, which in principle could play a similar role as the catalytic arginine by counteracting negative charge during the transition state of GTP hydrolysis.

### FURTHER VARIATIONS IN THE GTPASE MECHANISM

Another variation of the GTPase mechanism has been described for the dynamain-related Irga6 GTPase, which displays cooperative GTP hydrolysis and GTP-dependent oligomerization in solution.<sup>76</sup> Full-length crystal structures in the nucleotide-free and GDP-bound form revealed the basic architecture of the Irga6 GTPase, including a relatively small GTPase domain of  $\sim 200$  residues and an adjacent helical bundle formed by sequences N- and C-terminal of the GTPase domain.<sup>57</sup> Also a GMPPNP-bound crystal structure was obtained by soaking the nucleotide into nucleotide-free crystals. While this approach resulted in structural insights into GMPPNP binding, it did not allow large scale structural rearrangements of Irga6 molecules in the crystals; for example, in none of these crystals, the nucleotide-dependent G-interface was formed. Extensive mutagenesis data indicated that residues in the G-interface participate in the GTP hydrolysis mechanism.<sup>77</sup> Furthermore, Glu106 from the switch I regions was shown to be essential for catalysis. Unexpectedly, also the 3' OH of the ribose was demonstrated to be crucial for nucleotide-mediated assembly. A similar involvement of the 3' OH group was seen before for the signal recognition particle and its receptor, two GTPases which dimerize in an anti-parallel, head-to-tail fashion.<sup>78,79</sup> Consequently, an analogues head-to-tail dimerization mechanism was proposed for Irga6.

However, a recent structural analysis of a GMPPNP-bound non-oligomerizing Irga6 mutant, containing mutations outside the GTPase domain, indicates that also Irga6 dimerizes in a parallel head-to-head fashion, similar to all other dynamin superfamily proteins (Figure 2D).<sup>58</sup> In this moderate resolution structure, the switch I of Irga6 contacts the 2' and 3' OH groups of the ribose in the opposing protein. This contact, in turn, leads to the rearrangement of switch I and the repositioning of Glu106 toward the magnesium ion where it appears to replace the catalytic threonine from G2 in other GTPases (Figures 2A and 2D). Interestingly, Irga6 bears Gly79 at the third position in the P-loop. During catalysis, this glycine could form a main chain hydrogen bond to the bridging oxygen between the  $\beta$ - and  $\gamma$ -phosphates to stabilize the transition state of GTP hydrolysis. Alternatively, it may also be involved in the stabilization of a catalytic cation. Further structural analyses of Irga6 in the presence of a transition state mimic are required to unequivocally demonstrate the function of Gly79.

Not only dynamin superfamily proteins, but also septin GTPases<sup>80,81</sup> and septin-related GTPase, such as Toc34<sup>82</sup> and the GTPases of immunity-associated proteins (GIMAPs)<sup>83,84</sup> dimerize in a parallel head-to-head fashion and use related mechanisms of GTP hydrolysis. In fact, phylogenetic comparisons including analysis of the higher order assembly indicate that septins and dynamins originate from a common membrane-associated dimerizing ancestor.<sup>83</sup> Also other GTPases, such as the SRP or MnmE, use dimerization-dependent GTPase mechanisms.<sup>85,86</sup> However, their dimerization modes differ and they are phylogenetically not closely related to the dynamin superfamily within the GTPase phylogeny, suggesting a convergent evolution.

## CONTROL OF GTPASE DOMAIN DIMERIZATION

How is GTPase domain dimerization and thus, the GTPase function controlled to prevent futile cycles of GTP hydrolysis? Recent structural analyses of the auto-inhibited dynamin tetramer indicate that two of the four GTPase domains form intermolecular contacts to the PH domains of an adjacent dimer.<sup>49</sup> In this position, they are sterically restricted to engage in GTPase domains contacts. On membrane recruitment, the PH domains reposition toward the lipid surface and are therefore thought to release the auto-inhibitory contacts. Similar intermolecular auto-inhibitory contacts may exist for other dynamin superfamily proteins. For example, a monomeric MxA variant shows increased GTPase activity compared to its tetrameric wild-type counterpart.<sup>41</sup> In the auto-inhibited EHD2 dimer, a regulatory EH domain was shown to block the G-interface by delivering its C-terminal tail into the

nucleotide-binding site.<sup>37</sup> On membrane binding, the EH domain was proposed to be released from the GTPase domain to bind to interaction partners or to stabilize the EHD2 oligomer. Furthermore, the N-terminal eight residues of EHD2 were shown to fold back into a hydrophobic pocket of the GTPase domain (Figure 1C).<sup>60</sup> In the presence of membranes, the N-terminus switches into the lipid bilayer, as demonstrated by electron paramagnetic resonance studies. This switch appears to negatively control membrane binding, since an EHD2 variant without the N-terminus showed increased membrane recruitment in a fibroblast cell line.<sup>60</sup>

BDLP from the cyanobacterium *Nostoc punctiforme* does not show a lipid-stimulated GTPase reaction.<sup>26</sup> It bears a lysine residue at the third P-loop position. However, as many other bacteria, *Nostoc* strains have several dynamin-like proteins in their genomes, some of which contain a serine at the corresponding P-loop position. Accordingly, it has been speculated that heterodimerization with another member may control the GTPase function of these BDLPs.<sup>27,87</sup> Such a hypothesis is supported by the architecture of DynA from *Bacillus subtilis*, which is composed of a tandem of two BDLP units, both of which carrying a serine at position three in their P-loops. For this protein, cooperative GTP hydrolysis and interaction with membranes has been shown.<sup>27</sup> Also for IRGs, it has been demonstrated that one subfamily containing a GMS variation in the terminal sequence of their P-loops controls the GTPase function of the second subfamily via heterodimerization.<sup>88</sup>

## CONFORMATIONAL CHANGES INDUCED BY GTP HYDROLYSIS

How are the structural changes induced by GTP hydrolysis translated into a mechanical force? For a few dynamin superfamily proteins, full-length structures or structures of the GTPase domain and the adjacent helical domain were determined in different nucleotide-loading states and showed remarkable structural rearrangement on GTP hydrolysis and/or phosphate release. Interestingly, compared to the GTPase domain dimerization interface, these structural changes vary quite considerably between the different members.

Although no stable dimerization was found in solution for the dynamin-GG construct in the presence of GMPPCP and GDP,<sup>62</sup> dimeric crystal structures were obtained for these states, which were likely induced by the high protein concentration during crystallization.<sup>32,89</sup> The BSE adopts two strikingly different conformations relative to the GTPase domains, when comparing the GDP- and GDP-AlF<sub>4</sub><sup>-</sup>-bound forms to the GMPPCP-bound structure (Figure 3A): In the GDP-bound structure, the BSE tightly folds against the backside of the GTPase domain representing the closed conformation, whereas

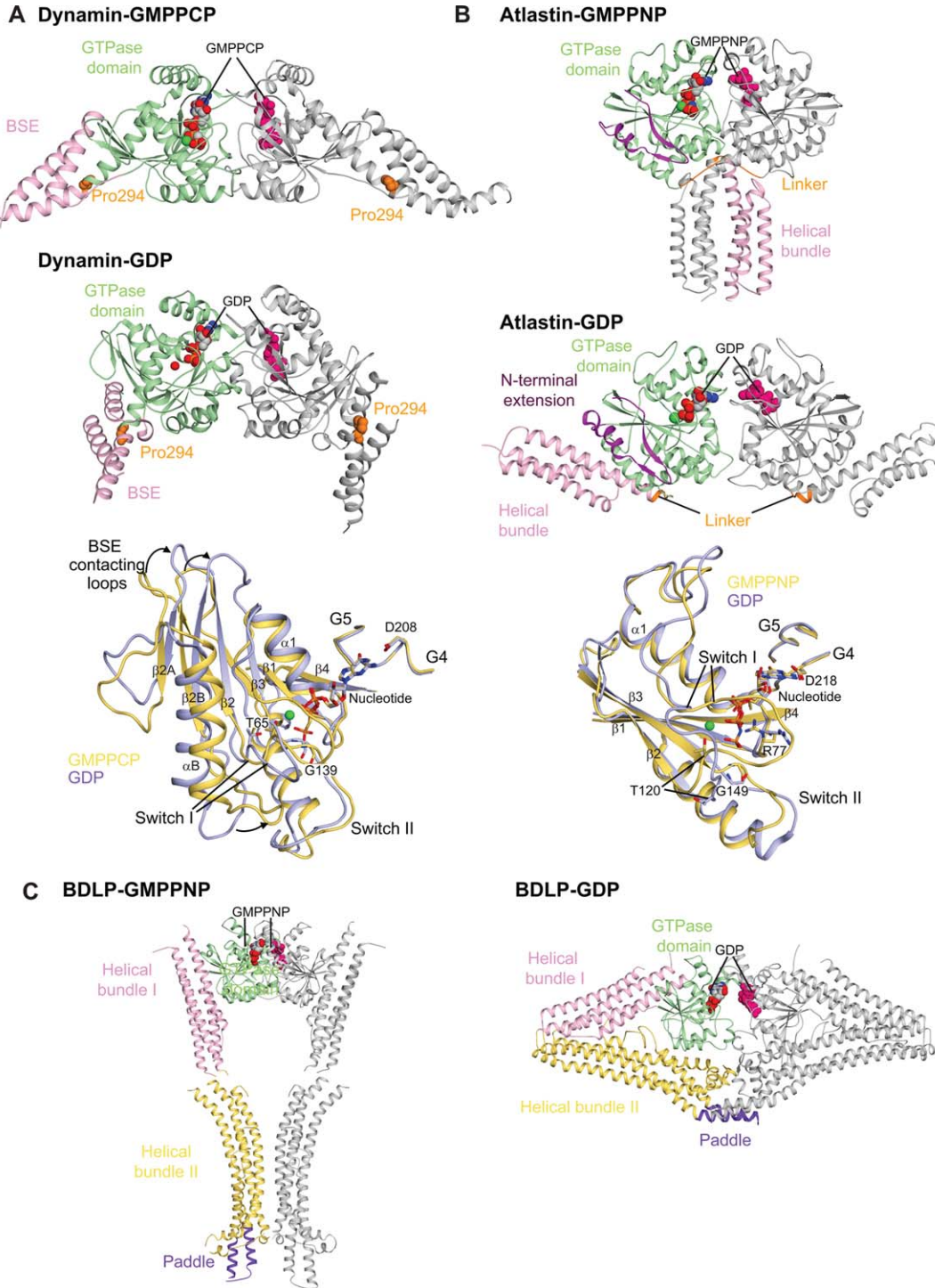


**FIGURE 3** Nucleotide- and/or lipid binding-induced structural changes in dynamin superfamily proteins. (A) GDP and GMPPCP-bound structures of dynamin dimers (pdbs 5D3Q, 3ZYC).<sup>32,89</sup> Note the large-scale rearrangement of the BSE versus the GTPase domains around a conserved hinge at Pro294 (orange). At the bottom, the two structures were superimposed along their guanine bases. For clarity, only the region encompassing  $\beta 1$ – $\beta 4$  is shown, and the G4 and G5 motifs. (B) Structure of atlantin in the GDP-bound (3Q5E)<sup>54</sup> and GMPPNP-bound forms (4IDP).<sup>56</sup> The superposition is shown in the same style as in A). (C) GDP-bound (pdb 2J68)<sup>26</sup> and GMPPNP-bound BDLP structures (2W6D).<sup>39</sup> The GMPPNP-bound structure was obtained by fitting the domains of the GDP-bound form into a cryo-EM reconstruction of BDLP oligomerized around a tubular membrane template. Accordingly, the detailed structural changes within the catalytic site could not be deduced.

in the GMPPNP-bound form, it is 70° rotated around the conserved Pro294 to adopt an open conformation. It has been suggested that the movement from the open to the closed conformation acts as a power stroke during membrane remodeling (see below).

What is the molecular basis for this movement? When comparing the GDP- and GMPPCP-bound structures, in particular switch I undergoes a dramatic rearrangement and helix  $\alpha 1$  in between the P-loop and switch I a slight rotation (Figure 3A). The latter rotation was suggested to lead to a tightening of hydrophobic residues in the GTPase domain core and a slight bending of the central  $\beta$ -sheet.<sup>32</sup> Consequently, two loop regions in the GTPase domain at the opposite side of the nucleotide rearrange. Together with residues of the central  $\beta$ -sheet, they mediate contacts to the first BSE helix and the adjacent linker in the closed, but not in the open conformation, and therefore control the nucleotide-dependent movement of the BSE. In addition, relaxation of the switch regions following GTP hydrolysis may allow the GTPase domain dimer to dissociate.

Similar to dynamin, an open and a closed conformation was obtained for the GMPPNP- and GDP-bound structures of an equivalent MxA-GG construct that dimerized in an analogous way via the G-interface.<sup>90</sup> Mutational studies confirmed that MxA employs a related mechanism of dimerization and GTP hydrolysis to dynamin which is required for its antiviral action.<sup>91</sup> For a GG construct of DNMI1L, an open BSE conformation was obtained for the GMPPCP and GDP- $\text{AlF}_4^-$ -bound dimeric forms,<sup>92</sup> whereas a closed conformation was obtained for the nucleotide-free monomeric form of the GG construct<sup>93</sup> and also for the nucleotide-free full-length structure.<sup>52</sup> Mutagenesis data suggested a related mechanism compared to dynamin.<sup>93</sup> Interestingly, an *Arabidopsis thaliana* dynamin-related protein 1A GG construct showed an open BSE in the GDP- $\text{AlF}_4^-$  bound form and a closed BSE in the presence of GDP.<sup>94</sup> Thus, whereas the crystallized GMPPNP/GMPPCP-bound forms of dynamin superfamily proteins always display an open and the GDP- and nucleotide-free forms always a closed BSE conformation, both open and closed BSE conformations are found for transition state mimics of GTP hydrolysis.

Also atlastin shows two fundamentally different conformations of the helical domain relative to the GTPase domains in the GMPPNP and GDP-bound structure, but the mode of the movement is completely different compared to dynamin (Figure 3B).<sup>54–56</sup> In the open GDP-bound form, the two helical domains protrude in opposite directions, with the GTPase domain dimer in the center. In the closed GMPPNP-bound conformation, the helical domains extend in parallel directions, cross over and therefore directly contact each other. Interestingly, the closed conformation was also obtained for a second GDP-bound crystal form, suggesting that the two con-

formations are of similar energy and can be stabilized by different crystal contacts.

A comparison of the GMPPNP- and GDP-structures shows that the two switch regions adopt completely different orientations (Figure 3B, bottom). This leads to a tightening of the GTPase domain interface in the GMPPNP versus the GDP-bound state which may promote the association of the two opposing helical domains in the GMPPNP-bound state. Furthermore, switch II directly contacts the linker between the GTPase domain and helical domain in both states and may convey the nucleotide-loading status directly to the helical domain. The catalytic Arg77 switches from the nucleotide in the GMPPNP-bound form toward the GTPase domain of the opposing dimer, possibly controlling the assembly of atlastin. Fluorescence resonance energy transfer measurements using a soluble construct comprising the GTPase domain and the helical bundle revealed the movements of these domains in response to nucleotide binding and hydrolysis.<sup>56</sup> Based on these experiments, a sequel of events leading to the tethering and fusion of opposing membranes was inferred. Efficient membrane fusion by atlastin also requires the C-terminal amphipathic helix which appears to perturb the membrane by inserting into the bilayer.<sup>95</sup> Unlike in many dynamin superfamily members, the helix does not seem to interact with other domains of the protein.

Similar to atlastin, conformational changes occurring during GTP hydrolysis of GBP1 are relayed within the LG-domain. As a result, the C-terminal helical domain was suggested to be released from the LG-domain during GTP hydrolysis to engage in coil-coiled interactions (see Figure 1B). Consequently, mutations of residues between the LG-domain and the helical domain or a deletion of the last two  $\alpha$ -helices in the helical domain resulted in increased GTPase activity.<sup>96</sup> Furthermore, the release of the contacts between the LG-domain and the C-terminal helices may lead to the formation of higher order oligomers<sup>97</sup> and allow the lipid-modified C-terminus to interact with lipid membranes.<sup>98</sup>

For BDLP, the GTPase domains dimerize via the G-interface in the GDP-bound form.<sup>26</sup> The two helical domains of each monomer are in a closed conformation, with a sharp kink in between the domains via a hinge region (Figure 3C, right). The tips of the two helical domains from opposing molecules contain the membrane binding “paddle” region and assemble with each other in a closed conformation. In the presence of GTP and liposomes, BDLP oligomerizes at the surface of liposomes leading to membrane tubulation. An 11 Å cryo EM reconstruction of this protein-lipid assembly revealed a dramatic domain opening of the two helical domains, which protrude in parallel orientations, with the paddle inserted into the membrane bilayer.<sup>39</sup> (Figure 3C, left) The GTPase domains

dimerize via the G-interface, but the packing of this interface appears to be tighter compared to the GDP-bound form. Due to the moderate resolution of the cryo EM reconstruction, it was not possible to deduce the detailed molecular mechanism how GTP-binding in combination with the membrane interaction can induce such dramatic domain rearrangements.

## HARNESSING THE ENERGY OF GTP HYDROLYSIS FOR A MECHANO-CHEMICAL FUNCTION

How is the energy of GTP hydrolysis exploited in the dynamin superfamily to perform mechano-chemical work on the membrane? From a theoretical point of view, the energy of hydrolyzing one GTP molecule to GDP yields about  $20 k_B T$ .<sup>99</sup> It has been proposed that this energy can be transformed with an efficiency of about 40% into mechanical force, and thus hydrolysis of only a few GTP molecules would provide sufficient energy to exceed the energy barrier required for membrane fission by constriction ( $35\text{--}70 k_B T$ ).<sup>99</sup> The energy barrier for fission further depends on the tension and rigidity of the membrane, which in vivo is influenced by the organization of certain lipid molecules and also other membrane interacting proteins besides dynamin.<sup>99</sup>

For dynamin, it has been shown that the stalk mediates the assembly of a right-handed nonconstricted helical filament with a preferred inner diameter of  $\sim 20$  nm corresponding roughly to the neck diameter of a clathrin-coated vesicle (Figure 4A).<sup>49</sup> Once the filament has fully embraced its tubular membrane template, GTP-bound GTPase domains are thought to dimerize across adjacent filaments.<sup>41,101</sup> It has been suggested that short dynamin collars comprised of only 13 dimers (corresponding to the formation of three G-interfaces across helical turns<sup>47</sup>) are sufficient to promote membrane fission in vitro<sup>102</sup> and in vivo.<sup>103,104</sup> In contrast, long dynamin collars at the neck of constricted pit have only been observed in cells if GTP-hydrolysis was blocked by mutations, addition of inhibitors or depletion of clathrin.<sup>10,29,105</sup>

On assembly, the power stroke derived from GTP hydrolysis may pull adjacent filaments along each other, resulting in constriction of the underlying membrane template. Consecutive rounds of GTP hydrolysis could sequentially increase membrane curvature. As constriction by the dynamin coat proceeds, the inner leaflets of the membrane are thought to fuse at a critical tubule diameter, achieving a hemifission intermediate.<sup>106,107</sup> Destabilization of the membrane seems to be the strongest at the edge of an assembled and constricted dynamin helical filament, where the change in membrane curvature is highest.<sup>99</sup> Completion of membrane fission may be promoted by membrane insertion of hydrophobic residues from the PH domain and the

dissociation of dynamin oligomers following GTP hydrolysis.<sup>102,107</sup> Such a fission mechanism may also apply to the close homologues DNM1L<sup>35,36,52</sup> and MxA, although the membrane-dependent function of the latter is unclear. Importantly, such membrane constriction mechanism strictly requires a helical arrangement of the dynamin filament, but it is not compatible with the ring-like arrangements observed under some in vitro conditions.<sup>108</sup> Conversely, ring-like oligomers could mediate the stabilization of certain membrane curvatures, as for example proposed for EHD oligomers at the neck of caveolae.<sup>37</sup>

In atlastin, it has been suggested that GTPase domain dimerization tethers opposing ER tubules (Figure 4B).<sup>54,55</sup> In this case, GTP hydrolysis may be required to pull opposing membranes toward each other by catalyzing the transition from the open to the cross-over helical conformation. Fusion of the closely juxtaposed membranes may then be further facilitated by disturbance of the lipids by TM-regions and the amphipathic helix in the C-terminal tail of atlastin.<sup>95,109</sup> In addition, it has been suggested that the GTPase function may be used to recycle atlastin dimers in the cross-over conformation back to the open conformation to allow new rounds of tethering across opposing membranes.<sup>110</sup> The exact role of GTPase hydrolysis and of the resulting conformational changes for membrane tethering and fusion are still controversially discussed.<sup>56,59,110,111</sup>

The close atlastin homologue GBP and the IRGs may use related mechanisms of mechano-chemical coupling, although molecular details how their innate immune function is linked to GTP-hydrolysis at the membrane are still sparse.<sup>20</sup> GBPs have recently been implicated in mediating autophagy and the activation of inflammasomes. In the case of IRG proteins, it has been shown that their GTP-dependent recruitment to the parasitophorous vacuole (PV) of *Toxoplasma gondii* is followed by rupture of the vacuole membrane.<sup>112</sup> Also, an accumulation of vesicles at the PV has been observed. Although these data imply that IRGs may actively destroy the integrity of the PV membrane, this hypothesis has not been formally proven. Recent publications indicate that the GBPs follow the IRGs to the PV and may cooperate with them in pathogen restriction in mice.<sup>113–115</sup> In humans, however, IRG proteins with an immune function are missing and GBPs are not recruited to the PV, despite their role in pathogen restriction.<sup>116</sup>

In bacteria, DynA is enriched at the septa of dividing cells suggesting a role in membrane fusion of the invaginating septum. For DynA, a vesicle tethering and fusion activity has been shown in vitro, which occurred independently of GTP-binding and hydrolysis.<sup>27</sup> As outlined above, BDLP shows GTP-dependent assembly on membranes resulting in the formation of a highly curved membrane tubule.<sup>26</sup> It has been suggested that these highly strained membrane tubules are fusogenic (Figure 4C). Following GTP hydrolysis and the removal of the

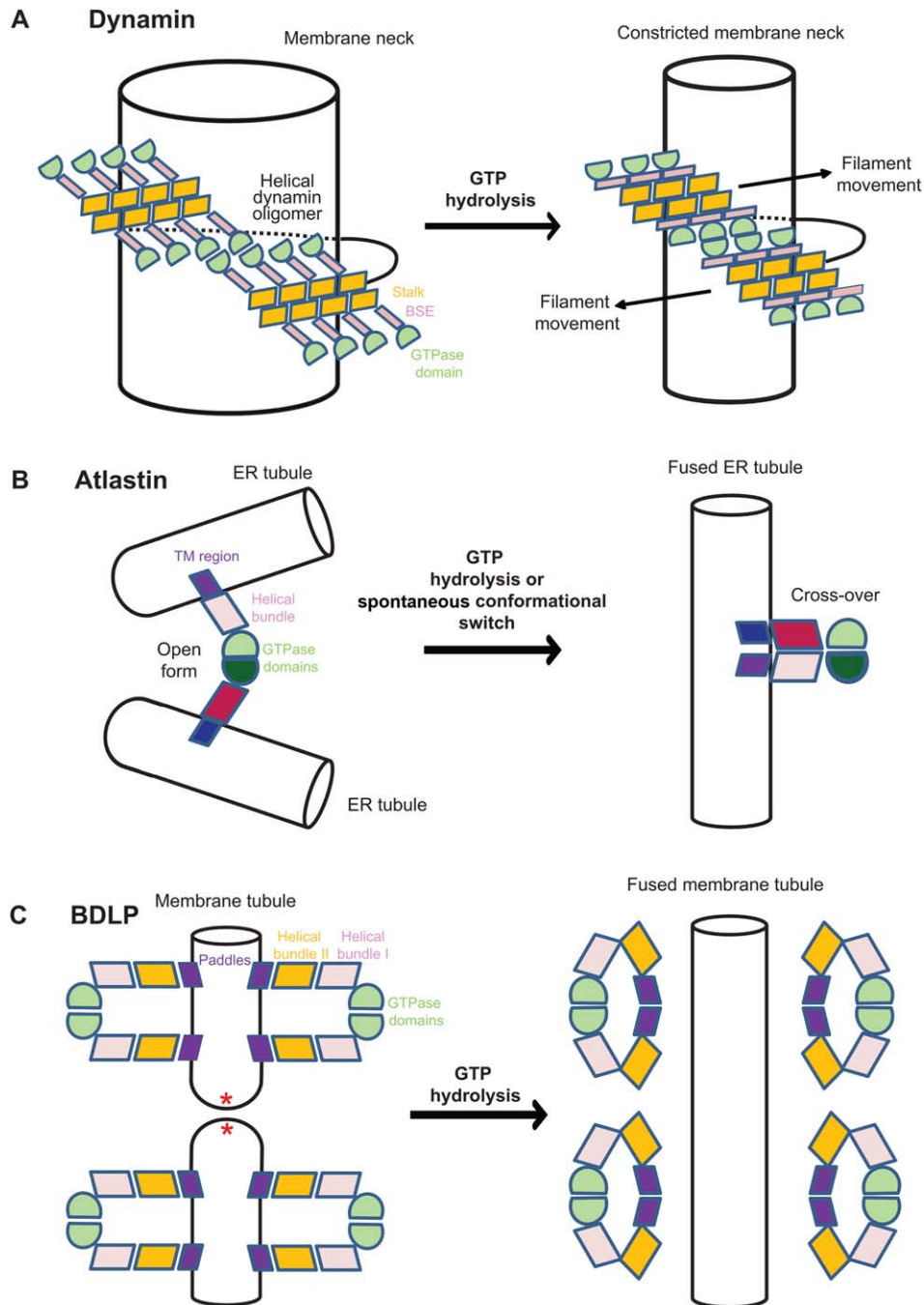


**FIGURE 4** Schematic models for the mechano-chemical action of dynamin superfamily proteins on membranes. The same domain colouring scheme as in Figures 1–3 is used (A) Constriction model of dynamin.<sup>100</sup> After PH-domain dependent recruitment to the membrane, a right-handed dynamin filament oligomerizes via the stalk around a tubular membrane template, like the neck of clathrin-coated vesicles. Once the filament has embraced the tubular membrane template, GTPase domains of adjacent helical turns dimerize. The GTPase-induced power stroke was suggested to pull adjacent filaments along each other (arrow) leading to constriction and eventually cleavage of the membrane tubule. For better clarity, the PH domains are not included in this graph. (B) Fusion model of atlastin. The GTPase domains of atlastin dimerize across ER tubules in the open conformation. Nucleotide hydrolysis-induced conformational changes catalyze the transition toward the cross-over conformation, thereby pulling the two membranes toward each other, leading to membrane fusion. Note that the indicated transmembrane domains (blue) were not present in the crystallized construct. (C) Fusion model of BDLP. In the GTP-bound form, BDLP oligomerizes in its open conformation on a membrane surface, thereby inducing and stabilizing membrane tubules of high curvature, probably by insertion of the paddle region. GTP hydrolysis converts BDLP back to the closed conformation which is released from the membrane, leaving behind highly strained membrane tubule, that are prone to undergo membrane fusion (according to Ref. 39).

BDLP coat, membrane tubules generated by BDLP were therefore proposed to undergo membrane fusion.<sup>39</sup> In this case, GTP-binding is thought to allow the assembly of the BDLP oligomer, and GTP hydrolysis the recycling of the oligomer back to the closed form.

The proposed model is in contrast to that of mitofusin, for which GTP-binding and hydrolysis occur at distinct points during membrane fusion (reviewed in Ref. 116). Furthermore, a mutational analysis showed that dimerization of Fzo1p from yeast requires GTP-binding and involves two residues in the P-loop, Asp195 and Asn197, the latter of which corresponds to the Arg48 in GBP1 and Ser41 in dynamin1, respectively.<sup>118</sup> The *cis* dimers of GTP-bound Fzo1p then interact *in trans* to tether mitochondrial outer membranes. It is not yet clear whether the *cis* or the *trans* dimers involve the G-interface. For efficient membrane fusion, Fzo1p has first to hydrolyze GTP to be then ubiquitinated by the F-Box protein Mdm30 and finally be degraded. This process seems at least partially conserved in mammals since a mutation in the P-loop of mitofusin2 was identified in Charcot-Marie-Tooth disease patients<sup>119</sup> and recently, it has been found that ubiquitinylation also controls the fusion activity of mitofusins.<sup>120</sup> The mechanism of mitochondrial inner membrane fusion by the OPA1/Mgm1p proteins is experimentally difficult to study and therefore less well understood. Both, OPA1 and Mgm1 proteins are present in the mitochondrial intermembrane space as long and short forms which are formed by mRNA splicing or proteolytic processing. These isoforms can form homo and hetero-oligomers and it has been proposed that the GTPase inactive long isoforms mediate tethering of the inner and out mitochondrial membranes while GTPase hydrolysis by the short isoforms drives the fusion process.<sup>66,121</sup>

## CONCLUSIONS

Since their initial discovery, dynamin superfamily proteins have witnessed growing attention as mechano-chemical enzymes mediating nucleotide-driven cellular membrane remodeling events. While initial biochemical and cell-based experiments, paired with reconstitution experiments and EM analyses, have resulted in initial models of dynamin action, the recent explosion of high resolution structural data have helped to understand the underlying mechanisms in molecular detail. The catalytic mechanisms of dynamin superfamily proteins have now been described for a number of cases. While their catalytic mechanism is related and phylogenetically conserved, details of catalysis differ between the various members and may be adapted to the specific cellular function. For dynamin, atlastin, and BDLP, the coupling between catalysis and the conformational movement of the adjacent helical domain has been inten-

sively characterized. For other members of the dynamin superfamily, this coupling is less well understood. Structures representing all nucleotide states along the reaction pathway combined with experiments to define the assembly state and dynamics in solution will help to clarify the mechanism of GTPase activation and the resulting conformational changes. The larger challenge will be the coupling of this process to membrane remodeling events. This is particularly the case for the dynamin-related proteins involved in membrane fusion events (mitofusins, OPA1/Mgm1p, atlastins, and bacterial dynamins). Their membrane interaction is mediated by trans-membrane or bilayer inserting helices. With the exception of BDLP,<sup>39</sup> we have currently no structural information about the conformation of these proteins on a membrane. As discussed for the SNARE proteins, the question has to be answered, if the helical domains extends into the lipid bilayer and induces perturbations of the lipids that destabilize the membrane<sup>122</sup> or if close tethering of membranes is sufficient for effective fusion.<sup>123</sup> Likewise, for the dynamin family members with antimicrobial and antiviral activity (Mx, GBPs, IRGs), future studies will have to address how the pathogen or the pathogen-containing compartments are identified and how the energy of GTP hydrolysis is utilized to interfere with the life-cycle of the pathogen.

## REFERENCES

1. Praefcke, G. J.; McMahon, H. T. *Nat Rev Mol Cell Biol* 2004, 5, 133–147.
2. Faelber, K.; Gao, S.; Held, M.; Posor, Y.; Haucke, V.; Noe, F.; Daumke, O. *Prog Mol Biol Transl Sci* 2013, 117, 411–443.
3. Staeheli, P.; Haller, O.; Boll, W.; Lindenmann, J.; Weissmann, C. *Cell* 1986, 44, 147–158.
4. Rothman, J. H.; Raymond, C. K.; Gilbert, T.; O'Hara, P. J.; Stevens, T.H. *Cell* 1990, 61, 1063–1074.
5. Shpetner, H. S.; Vallee, R. B. *Cell* 1989, 59, 421–432.
6. Obar, R. A.; Collins, C. A.; Hammarback, J. A.; Shpetner, H. S.; Vallee, R. B. *Nature* 1990, 347, 256–261.
7. van der Bliek, A. M.; Meyerowitz, E. M. *Nature* 1991, 351, 411–414.
8. Chen, M. S.; Obar, R. A.; Schroeder, C. C.; Austin, T. W.; Poodry, C. A.; Wadsworth, S. C.; Vallee, R. B. *Nature* 1991, 351, 583–586.
9. Poodry, C. A.; Hall, L.; Suzuki, D. T. *Dev Biol* 1973, 32, 373–386.
10. Koenig, J. H.; Ikeda, K. J. *Neuroscience* 1989, 9, 3844–3860.
11. Ferguson, S. M.; De Camilli, P. *Nat Rev Mol Cell Biol* 2012, 13, 75–88.
12. Smirnova, E.; Griparic, L.; Shurland, D. L.; van der Bliek, A. M. *Mol Biol Cell* 2001, 12, 2245–2256.
13. Alexander, C.; Votruba, M.; Pesch, U. E.; Thiselton, D. L.; Mayer, S.; Moore, A.; Rodriguez, M.; Kellner, U.; Leo-Kottler, B.; Auburger, G.; Bhattacharya, S. S.; Wissinger, B. *Nat Genet* 2000, 26, 211–215.
14. Delettre, C.; Lenaers, G.; Griffoin, J. M.; Gigarel, N.; Lorenzo, C.; Belenger, P.; Pelloquin, L.; Grosgeorge, J.; Turc-Carel, C.; Perret,

- E.; Astarie-Dequeker, C.; Lasquelles, L.; Arnaud, B.; Ducommun, B.; Kaplan, J.; Hamel, C. P. *Nat Genet* 2000, 26, 207–210.
15. Wong, E. D.; Wagner, J. A.; Gorsich, S. W.; McCaffery, J. M.; Shaw, J. M.; Nunnari, J. *J Cell Biol* 2000, 151, 341–352.
  16. Frezza, C.; Cipolat, S.; Martins de, B. O.; Micaroni, M.; Beznoussenko, G. V.; Rudka, T.; Bartoli, D.; Polishuck, R. S.; Danial, N. N.; De, S. B.; Scorrano, L. *Cell* 2006, 126, 177–189.
  17. Hales, K. G.; Fuller, M. T. *Cell* 1997, 90, 121–129.
  18. Santel, A.; Fuller, M. T. *J Cell Sci* 2001, 114, 867–874.
  19. Boehm, U.; Guethlein, L.; Klamp, T.; Ozbek, K.; Schaub, A.; Futterer, A.; Pfeffer, K.; Howard, J. C. *J Immunol* 1998, 161, 6715–6723.
  20. Meunier, E.; Broz, P. *Cell Microbiol* 2016, 18, 168–180.
  21. Vestal, D. J.; Jeyaratnam, J. A. *J Interferon Cytokine Res* 2011, 31, 89–97.
  22. Martens, S.; Parvanova, I.; Zerrahn, J.; Griffiths, G.; Schell, G.; Reichmann, G.; Howard, J. C. *PLoS Pathog* 2005, 1, e24.
  23. Orso, G.; Pendin, D.; Liu, S.; Tosetto, J.; Moss, T. J.; Faust, J. E.; Micaroni, M.; Egorov, A.; Martinuzzi, A.; McNew, J. A.; Daga, A. *Nature* 2009, 460, 978–983.
  24. Hu, J.; Shibata, Y.; Zhu, P. P.; Voss, C.; Rismanchi, N.; Prinz, W. A.; Rapoport, T. A.; Blackstone, C. *Cell* 2009, 138, 549–561.
  25. Naslavsky, N.; Caplan, S. *Trends Cell Biol* 2011, 21, 122–131.
  26. Low, H. H.; Lowe, J. *Nature* 2006, 444, 766–769.
  27. Burmann, F.; Ebert, N.; van, B. S.; Bramkamp, M. *Mol Microbiol* 2011, 79, 1294–1304.
  28. Michie, K. A.; Boysen, A.; Low, H. H.; Moller-Jensen, J.; Lowe, J. *PLoS One* 2014, 9, e107211.
  29. Takei, K.; McPherson, P. S.; Schmid, S. L.; De Camilli, P. *Nature* 1995, 374, 186–190.
  30. Hinshaw, J. E.; Schmid, S. L. *Nature* 1995, 374, 190–192.
  31. Stowell, M. H.; Marks, B.; Wigge, P.; McMahan, H. T. *Nat Cell Biol* 1999, 1, 27–32.
  32. Chappie, J. S.; Mears, J. A.; Fang, S.; Leonard, M.; Schmid, S. L.; Milligan, R. A.; Hinshaw, J. E.; Dyda, F. *Cell* 2011, 147, 209–222.
  33. Accola, M. A.; Huang, B.; Al, M. A.; McNiven, M. A. *J Biol Chem* 2002, 277, 21829–21835.
  34. von der Malsburg, A.; Abutbul-Ionita, I.; Haller, O.; Kochs, G.; Danino, D. *J Biol Chem* 2011, 286, 37858–37865.
  35. Ingerman, E.; Perkins, E. M.; Marino, M.; Mears, J. A.; McCaffery, J. M.; Hinshaw, J. E.; Nunnari, J. *J Cell Biol* 2005, 170, 1021–1027.
  36. Mears, J. A.; Lackner, L. L.; Fang, S.; Ingerman, E.; Nunnari, J.; Hinshaw, J. E. *Nat Struct Mol Biol* 2011, 18, 20–26.
  37. Daumke, O.; Lundmark, R.; Vallis, Y.; Martens, S.; Butler, P. J.; McMahan, H. T. *Nature* 2007, 449, 923–927.
  38. Ban, T.; Heymann, J. A.; Song, Z.; Hinshaw, J. E.; Chan, D. C. *Hum Mol Genet* 2010, 19, 2113–2122.
  39. Low, H. H.; Sachse, C.; Amos, L. A.; Lowe, J. *Cell* 2009, 139, 1342–1352.
  40. Warnock, D. E.; Hinshaw, J. E.; Schmid, S. L. *J Biol Chem* 1996, 271, 22310–22314.
  41. Gao, S.; von der Malsburg, A.; Paeschke, S.; Behlke, J.; Haller, O.; Kochs, G.; Daumke, O. *Nature* 2010, 465, 502–506.
  42. Ghosh, A.; Praefcke, G. J.; Renault, L.; Wittinghofer, A.; Herrmann, C. *Nature* 2006, 440, 101–104.
  43. Tuma, P. L.; Collins, C. A. *J Biol Chem* 1994, 269, 30842–30847.
  44. Prakash, B.; Praefcke, G. J.; Renault, L.; Wittinghofer, A.; Herrmann, C. *Nature* 2000, 403, 567–571.
  45. Praefcke, G. J.; Kloep, S.; Benscheld, U.; Lilie, H.; Prakash, B.; Herrmann, C. *J Mol Biol* 2004, 344, 257–269.
  46. Tuma, P. L.; Stachniak, M. C.; Collins, C. A. *J Biol Chem* 1993, 268, 17240–17246.
  47. Faelber, K.; Posor, Y.; Gao, S.; Held, M.; Roske, Y.; Schulze, D.; Haucke, V.; Noe, F.; Daumke, O. *Nature* 2011, 477, 556–560.
  48. Ford, M. G.; Jenni, S.; Nunnari, J. *Nature* 2011, 477, 561–566.
  49. Reubold, T. F.; Faelber, K.; Plattner, N.; Posor, Y.; Ketel, K.; Curth, U.; Schlegel, J.; Anand, R.; Manstein, D. J.; Noe, F.; Haucke, V.; Daumke, O.; Eschenburg, S. *Nature* 2015, 525, 404–408.
  50. Gao, S.; von der, M. A.; Dick, A.; Faelber, K.; Schroder, G. F.; Haller, O.; Kochs, G.; Daumke, O. *Immunity* 2011, 35, 514–525.
  51. Fribourgh, J. L.; Nguyen, H. C.; Matreyek, K. A.; Alvarez, F. J.; Summers, B. J.; Dewdney, T. G.; Aiken, C.; Zhang, P.; Engelman, A.; Xiong, Y. *Cell Host Microbe* 2014, 16, 627–638.
  52. Frohlich, C.; Grabiger, S.; Schwefel, D.; Faelber, K.; Rosenbaum, E.; Mears, J.; Rocks, O.; Daumke, O. *EMBO J* 2013, 32, 1280–1292.
  53. Prakash, B.; Renault, L.; Praefcke, G. J.; Herrmann, C.; Wittinghofer, A. *EMBO J* 2000, 19, 4555–4564.
  54. Byrnes, L. J.; Sondermann, H. *Proc Natl Acad Sci USA* 2011, 108, 2216–2221.
  55. Bian, X.; Klemm, R. W.; Liu, T. Y.; Zhang, M.; Sun, S.; Sui, X.; Liu, X.; Rapoport, T. A.; Hu, J. *Proc Natl Acad Sci USA* 2011, 108, 3976–3981.
  56. Byrnes, L. J.; Singh, A.; Szeto, K.; Benven, N. M.; O'Donnell, J. P.; Zipfel, W. R.; Sondermann, H. *EMBO J* 2013, 32, 369–384.
  57. Ghosh, A.; Uthaiyah, R.; Howard, J.; Herrmann, C.; Wolf, E. *Mol Cell* 2004, 15, 727–739.
  58. Schulte, K.; Pawlowski, N.; Faelber, K.; Frohlich, C.; Howard, J.; Daumke, O. *BMC Biol* 2016, 14, 14.
  59. Yan, L.; Sun, S.; Wang, W.; Shi, J.; Hu, X.; Wang, S.; Su, D.; Rao, Z.; Hu, J.; Lou, Z. *J Cell Biol* 2015, 210, 961–972.
  60. Shah, C.; Hegde, B. G.; Moren, B.; Behrmann, E.; Mielke, T.; Moenke, G.; Spahn, C. M.; Lundmark, R.; Daumke, O.; Langen, R. *Structure* 2014, 22, 409–420.
  61. Niemann, H. H.; Knetsch, M. L.; Scherer, A.; Manstein, D. J.; Kull, F. J. *EMBO J* 2001, 20, 5813–5821.
  62. Chappie, J. S.; Acharya, S.; Leonard, M.; Schmid, S. L.; Dyda, F. *Nature* 2010, 465, 435–440.
  63. Saraste, M.; Sibbald, P. R.; Wittinghofer, A. *Trends Biochem Sci* 1990, 15, 430–434.
  64. Praefcke, G. J.; Geyer, M.; Schwemmle, M.; Kalbitzer, H. R.; Herrmann, C. *J Mol Biol* 1999, 292, 321–332.
  65. Bustillo-Zabalbeitia, I.; Montessuit, S.; Raemy, E.; Basanez, G.; Terrones, O.; Martinou, J. C. *PLoS One* 2014, 9, e102738.
  66. DeVay, R. M.; Dominguez-Ramirez, L.; Lackner, L. L.; Hoppins, S.; Stahlberg, H.; Nunnari, J. *J Cell Biol* 2009, 186, 793–803.
  67. Meglei, G.; McQuibban, G. A. *Biochemistry* 2009, 48, 1774–1784.
  68. Daumke, O.; Roux, A.; Haucke, V. *Cell* 2014, 156, 882–892.
  69. Schwemmle, M.; Staeheli, P. *J Biol Chem* 1994, 269, 11299–11305.
  70. Kunzelmann, S.; Praefcke, G. J.; Herrmann, C. *J Biol Chem* 2006, 281, 28627–28635.
  71. Wehner, M.; Kunzelmann, S.; Herrmann, C. *FEBS J* 2012, 279, 203–210.
  72. Marks, B.; Stowell, M. H.; Vallis, Y.; Mills, I. G.; Gibson, A.; Hopkins, C. R.; McMahan, H. T. *Nature* 2001, 410, 231–235.
  73. Scrima, A.; Wittinghofer, A. *EMBO J* 2006, 25, 2940–2951.

74. Ash, M. R.; Maher, M. J.; Mitchell, G. J.; Jormakka, M. *FEBS Lett* 2012, 586, 2218–2224.
75. Lomash, R. M.; Gu, X.; Youle, R. J.; Lu, W.; Roche, K. W. *Cell Rep* 2015, 12, 743–751.
76. Uthaiiah, R. C.; Praefcke, G. J.; Howard, J. C.; Herrmann, C. *J Biol Chem* 2003, 278, 29336–29343.
77. Pawlowski, N.; Khaminets, A.; Hunn, J. P.; Papic, N.; Schmidt, A.; Uthaiiah, R. C.; Lange, R.; Vopper, G.; Martens, S.; Wolf, E.; Howard, J. C. *BMC Biol* 2011, 9, 7.
78. Egea, P. F.; Shan, S. O.; Napetschnig, J.; Savage, D. F.; Walter, P.; Stroud, R. M. *Nature* 2004, 427, 215–221.
79. Focia, P. J.; Shepotinovskaya, I. V.; Seidler, J. A.; Freymann, D. M. *Science* 2004, 303, 373–377.
80. Sirajuddin, M.; Farkasovsky, M.; Hauer, F.; Kuhlmann, D.; Macara, I. G.; Weyand, M.; Stark, H.; Wittinghofer, A. *Nature* 2007, 449, 311–315.
81. Sirajuddin, M.; Farkasovsky, M.; Zent, E.; Wittinghofer, A. *Proc Natl Acad Sci USA* 2009, 106, 16592–16597.
82. Sun, Y. J.; Forouhar, F.; Li Hm, H. M.; Tu, S. L.; Yeh, Y. H.; Kao, S.; Shr, H. L.; Chou, C. C.; Chen, C.; Hsiao, C. D. *Nat Struct Biol* 2002, 9, 95–100.
83. Schwefel, D.; Frohlich, C.; Eichhorst, J.; Wiesner, B.; Behlke, J.; Aravind, L.; Daumke, O. *Proc Natl Acad Sci USA* 2010, 107, 20299–20304.
84. Schwefel, D.; Arasu, B. S.; Marino, S. F.; Lamprecht, B.; Kochert, K.; Rosenbaum, E.; Eichhorst, J.; Wiesner, B.; Behlke, J.; Rocks, O.; Mathas, S.; Daumke, O. *Structure* 2013, 21, 550–559.
85. Gasper, R.; Meyer, S.; Gotthardt, K.; Sirajuddin, M.; Wittinghofer, A. *Nat Rev Mol Cell Biol* 2009, 10, 423–429.
86. Anand, B.; Majumdar, S.; Prakash, B. *Biochemistry* 2013, 52, 1122–1130.
87. Bramkamp, M. *Biol Chem* 2012, 393, 1203–1214.
88. Hunn, J. P.; Koenen-Waisman, S.; Papic, N.; Schroeder, N.; Pawlowski, N.; Lange, R.; Kaiser, F.; Zerrahn, J.; Martens, S.; Howard, J. C. *EMBO J* 2008, 27, 2495–2509.
89. Anand, R.; Eschenburg, S.; Reubold, T. F. *Biochem Biophys Res Commun* 2016, 469, 76–80.
90. Rennie, M. L.; McKelvie, S. A.; Bulloch, E. M.; Kingston, R. L. *Structure* 2014, 22, 1433–1445.
91. Dick, A.; Graf, L.; Olal, D.; von der, M. A.; Gao, S.; Kochs, G.; Daumke, O. *J Biol Chem* 2015, 290, 12779–12792.
92. Kishida, H.; Sugio, S. *Curr Top Pept Protein Res* 2013, 14, 67.
93. Wenger, J.; Klinglmayr, E.; Frohlich, C.; Eibl, C.; Gimeno, A.; Hessenberger, M.; Puehringer, S.; Daumke, O.; Goettig, P. *PLoS One* 2013, 8, e71835.
94. Yan, L.; Ma, Y.; Sun, Y.; Gao, J.; Chen, X.; Liu, J.; Wang, C.; Rao, Z.; Lou, Z. *J Mol Cell Biol* 2011, 3, 378–381.
95. Liu, T. Y.; Bian, X.; Sun, S.; Hu, X.; Klemm, R. W.; Prinz, W. A.; Rapoport, T. A.; Hu, J. *Proc Natl Acad Sci USA* 2012, 109, E2146–E2154.
96. Vopel, T.; Syguda, A.; Britzen-Laurent, N.; Kunzelmann, S.; Ludemann, M. B.; Dovengerds, C.; Sturzl, M.; Herrmann, C. *J Mol Biol* 2010, 400, 63–70.
97. Vopel, T.; Hengstenberg, C. S.; Peulen, T. O.; Ajaj, Y.; Seidel, C. A.; Herrmann, C.; Klare, J. P. *Biochemistry* 2014, 53, 4590–4600.
98. Fres, J. M.; Muller, S.; Praefcke, G. J. *J Lipid Res* 2010, 51, 2454–2459.
99. Morlot, S.; Galli, V.; Klein, M.; Chiaruttini, N.; Manzi, J.; Humbert, F.; Dinis, L.; Lenz, M.; Cappello, G.; Roux, A. *Cell* 2012, 151, 619–629.
100. Sweitzer, S. M.; Hinshaw, J. E. *Cell* 1998, 93, 1021–1029.
101. Mears, J. A.; Ray, P.; Hinshaw, J. E. *Structure* 2007, 15, 1190–1202.
102. Shnyrova, A. V.; Bashkurov, P. V.; Akimov, S. A.; Pucadyil, T. J.; Zimmerberg, J.; Schmid, S. L.; Frolov, V. A. *Science* 2013, 339, 1433–1436.
103. Cocucci, E.; Gaudin, R.; Kirchhausen, T. *Mol Biol Cell* 2014, 25, 3595–3609.
104. Grassart, A.; Cheng, A. T.; Hong, S. H.; Zhang, F.; Zenzer, N.; Feng, Y.; Briner, D. M.; Davis, G. D.; Malkov, D.; Drubin, D. G. *J Cell Biol* 2014, 205, 721–735.
105. Iversen, T. G.; Skretting, G.; van, D. B.; Sandvig, K. *Proc Natl Acad Sci USA* 2003, 100, 5175–5180.
106. Morlot, S.; Roux, A. *Annu Rev Biophys* 2013, 42, 629–649.
107. Mattila, J. P.; Shnyrova, A. V.; Sundborger, A. C.; Hortelano, E. R.; Fuhrmans, M.; Neumann, S.; Muller, M.; Hinshaw, J. E.; Schmid, S. L.; Frolov, V. A. *Nature* 2015, 524, 109–113.
108. Klockow, B.; Tichelaar, W.; Madden, D. R.; Niemann, H. H.; Akiba, T.; Hirose, K.; Manstein, D. J. *EMBO J* 2002, 21, 240–250.
109. Faust, J. E.; Desai, T.; Verma, A.; Ulengin, I.; Sun, T. L.; Moss, T. J.; Betancourt-Solis, M. A.; Huang, H. W.; Lee, T.; McNew, J. A. *J Biol Chem* 2015, 290, 4772–4783.
110. Liu, T. Y.; Bian, X.; Romano, F. B.; Shemesh, T.; Rapoport, T. A.; Hu, J. *Proc Natl Acad Sci USA* 2015, 112, E1851–E1860.
111. Saini, S. G.; Liu, C.; Zhang, P.; Lee, T. H. *Mol Biol Cell* 2014, 25, 3942–3953.
112. Zhao, Y. O.; Khaminets, A.; Hunn, J. P.; Howard, J. C. *PLoS Pathog* 2009, 5, e1000288.
113. Haldar, A. K.; Saka, H. A.; Piro, A. S.; Dunn, J. D.; Henry, S. C.; Taylor, G. A.; Frickel, E. M.; Valdivia, R. H.; Coers, J. *PLoS Pathog* 2013, 9, e1003414.
114. Haldar, A. K.; Foltz, C.; Finethy, R.; Piro, A. S.; Feeley, E. M.; Pilla-Moffett, D. M.; Komatsu, M.; Frickel, E. M.; Coers, J. *Proc Natl Acad Sci USA* 2015, 112, E5628–E5637.
115. Kravets, E.; Degrandi, D.; Ma, Q.; Peulen, T. O.; Klumpers, V.; Felekyan, S.; Kuhnemuth, R.; Weidtkamp-Peters, S.; Seidel, C. A.; Pfeffer, K. *Elife* 2016, 5,
116. Johnston, A. C.; Piro, A.; Clough, B.; Siew, M.; Virreira, W. S.; Coers, J.; Frickel, E. M. *Cell Microbiol* 2016. doi: 10.1111/cmi.12579 (ahead of print)
117. Escobar-Henriques, M.; Anton, F. *Biochim Biophys Acta* 2013, 1833, 162–175.
118. Anton, F.; Fres, J. M.; Schauss, A.; Pinson, B.; Praefcke, G. J.; Langer, T.; Escobar-Henriques, M. *J Cell Sci* 2011, 124, 1126–1135.
119. Detmer, S. A.; Chan, D. C. *J Cell Biol* 2007, 176, 405–414.
120. Yue, W.; Chen, Z.; Liu, H.; Yan, C.; Chen, M.; Feng, D.; Yan, C.; Wu, H.; Du, L.; Wang, Y.; Liu, J.; Huang, X.; Xia, L.; Liu, L.; Wang, X.; Jin, H.; Wang, J.; Song, Z.; Hao, X.; Chen, Q. *Cell Res* 2014, 24, 482–496.
121. Zick, M.; Duvezin-Caubet, S.; Schafer, A.; Vogel, F.; Neupert, W.; Reichert, A. S. *FEBS Lett* 2009, 583, 2237–2243.
122. Stein, A.; Weber, G.; Wahl, M. C.; Jahn, R. *Nature* 2009, 460, 525–528.
123. Xu, H.; Zick, M.; Wickner, W. T.; Jun, Y. *Proc Natl Acad Sci USA* 2011, 108, 17325–17330.

*Reviewing Editor: Alfred Wittinghofer*